



Rapid purification and crystal structure analysis of a small protein carrying two terminal affinity tags

Uwe Mueller^{1,2}, Konrad Büsow^{3,4}, Anne Diehl⁵, Franz J. Bartl⁶, Frank H. Niesen^{4,6}, Lajos Nyarsik³ & Udo Heinemann^{1,7,*}

¹Institut für Chemie/Kristallographie, Freie Universität Berlin, Takustr. 6, D-14195 Berlin, Germany; ²Protein Structure Factory, c/o BESSY GmbH, Albert-Einstein-Str. 15, D-12489 Berlin, Germany; ³Max-Planck-Institut für Molekulare Genetik, Ihnestr. 73, D-14195 Berlin, Germany; ⁴Protein Structure Factory, Heubnerweg 6, D-14059 Berlin, Germany; ⁵Forschungsinstitut für Molekulare Pharmakologie, Robert-Rössle-Str. 10, D-13125 Berlin, Germany; ⁶Institut für Medizinische Physik und Biophysik, Charité, Humboldt-Universität zu Berlin, Ziegelstr. 5-9, D-10098 Berlin, Germany; ⁷FG Kristallographie, Max-Delbrück-Centrum für Molekulare Medizin, Robert-Rössle-Str. 10, D-13125 Berlin, Germany; *Author for correspondence (Fax: +49-30-9406-2548; e-mail: heinemann@mdc-berlin.de)

Received 16 December 2002; accepted 19 August 2003

Key words: affinity chromatography, protein purification, SH3 domain, structural genomics, X-ray crystallography

Abstract

Small peptide tags are often fused to proteins to allow their affinity purification in high-throughput structure analysis schemes. To assess the compatibility of small peptide tags with protein crystallization and to examine if the tags alter the three-dimensional structure, the N-terminus of the chicken α -spectrin SH3 domain was labeled with a His₆ tag and the C-terminus with a StrepII tag. The resulting protein, His₆-SH3-StrepII, consists of 83 amino-acid residues, 23 of which originate from the tags. His₆-SH3-StrepII is readily purified by dual affinity chromatography, has very similar biophysical characteristics as the untagged protein domain and crystallizes readily from a number of sparse-matrix screen conditions. The crystal structure analysis at 2.3 Å resolution proves native-like structure of His₆-SH3-StrepII and shows the entire His₆ tag and part of the StrepII tag to be disordered in the crystal. Obviously, the fused affinity tags did not interfere with crystallization and structure analysis and did not change the protein structure. From the extreme case of His₆-SH3-StrepII, where affinity tags represent 27% of the total fusion protein mass, we extrapolate that protein constructs with N- and C-terminal peptide tags may lend themselves to biophysical and structural investigations in high-throughput regimes.

Abbreviations: SH3 domain – Src homology 3 domain; His₆-SH3-StrepII – α -spectrin SH3 domain with N-terminal His₆ and C-terminal StrepII affinity tag; GST – glutathione S-transferase; MBP – maltose-binding protein; aa – amino acid(s); rms – root-mean-square; MC – metal-chelating.

Introduction

The recombinant production of milligram quantities of pure and biologically active samples is a prerequisite for protein structure analysis by both X-ray crystallography and NMR spectroscopy. It is often the rate-limiting step in the structure-analysis process. The use of affinity tags N- and/or C-terminally fused

to the protein chain significantly facilitates protein purification. Affinity tags allow purification schemes to be designed in a way that is largely independent of the physical properties of the protein under investigation, since the interaction of the fusion protein with chromatography resins is dictated by the tag and not the protein itself. This is of utmost importance in high-throughput protein structure analysis schemes as

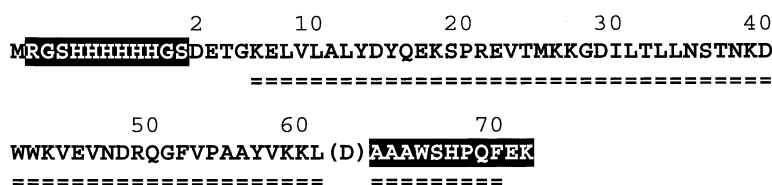


Figure 1. Amino-acid sequence of His₆-SH3-StrepII. Residues in normal print belong to the chicken α -spectrin SH3 domain, those in inverted print belong to the tags. The C-terminal Asp of the SH3 domain is enclosed in parentheses to indicate that this residue was lost in the cloning procedure. The underlined residues were observed in the electron density.

pursued in structural genomics programs [1–7] and commercial settings [7–9], where many proteins are being purified in parallel and the design of purification procedures exploiting the biophysical peculiarities of individual proteins would not be feasible.

One may discriminate between two types of affinity tags. Whole-protein tags (glutathione S-transferase (GST), maltose-binding protein (MBP), etc.) are usually removed proteolytically before crystallization or NMR analysis, although there have been occasional reports on their beneficial effects on protein solubility and crystallizability [10]. Peptide tags (oligohistidine (e.g., His₆), Strep, Flag, etc.) may be either cleaved off or retained on the protein after purification and before structure analysis. In either case, the removal of the affinity tag by cleavage with a site-specific or site-preferential protease such as thrombin, enterokinase, etc. is an additional preparative step. Furthermore, additional residues originating from the cloning and processing procedure may be left attached N- or C-terminally to the purified protein. There is always concern that the cleavage may remain incomplete or that unwanted proteolysis may occur at susceptible sites of the target protein.

For the recombinant production of human proteins in *Escherichia coli*, *Saccharomyces cerevisiae* or *Pichia pastoris* we are exploring a cloning strategy that produces proteins with an N-terminal His₆ tag and a C-terminal StrepII tag [11, 12]. Two different affinity tags are employed, since we have observed that the exclusive use of either one of them often results in incomplete purification necessitating further chromatography. Furthermore, a N-terminal tag may ensure proper translation initiation whereas an additional C-terminal tag allows for easy removal of incomplete translation products that will not bind to the cognate affinity resin. The subsequent structure analysis would be ideally performed in the presence of these tags to avoid the above-mentioned potential complications arising from proteolysis.

We are thus faced with the questions if (a) the affinity tags are compatible with crystallization and structure analysis and (b) they influence the three-dimensional protein structure. To address these questions, we have constructed a polypeptide, His₆-SH3-StrepII, consisting of the 60-aa Src homology-3 domain (SH3) of chicken α -spectrin [13] fused N-terminally to a His₆ tag [14] and C-terminally to a StrepII tag [15, 16] (Figure 1). The possible detrimental effects of the affinity tags on structure analysis and native-like conformation of this SH3 domain would be expected to be pronounced, since the two tags represent more than one fourth of the total fusion protein mass. It is shown that His₆-SH3-StrepII is easily purified to homogeneity by double-affinity chromatography over Ni-chelate and streptavidin columns, can be crystallized under various conditions, and has biophysical properties and a crystal structure similar to the unlabeled SH3 domain [13].

Material and methods

Plasmid construction

A cDNA fragment encoding the SH3 domain was PCR-amplified from the plasmid pET-SH3, obtained from the late M. Saraste (EMBL, Heidelberg), with the primers SH3-chick-U (5'-GGGGATCCGATGAAACTGGAAAAGAGCTTGTGC-3') and SH3-chick-L (5'-GGATGGATGCGGCCGCTAGTTTTTTCACATAGGCAGCTGG-3'). The product was then cloned between the *Bam*HI and *Not*I sites of pQStrep2, a modified form of the pQE-30 expression vector (Qiagen, Genbank accession no. AY028642). pQStrep2 provides for a N-terminal His₆ tag and a C-terminal StrepII tag [16]. The helper plasmid pSE111 was obtained from Dr. E. Scherzinger (Berlin) and carries the *lacI*^Q repressor and the *argU* gene for a rare tRNA.

Protein fermentation and purification

Two 500 ml LB cultures of *E. coli* BL21(DE3) pQStrep2 (carrying the gene for SH3 and encoding ampicillin resistance) pSE111, supplemented with 50 µg/ml ampicillin and 25 µg/ml kanamycin, were grown at 37 °C to an optical density of 0.8 at 600 nm. The culture was then induced with 1 mM IPTG. Two hours later the cells (OD₆₀₀ 2.0) were collected and washed with physiological salt solution. The cell pellet (4.4 g wet mass) was resuspended in 25 ml buffer A (20 mM Tris/HCl pH 8.0, 500 mM NaCl, 5 mM imidazole). The cells were desintegrated by two passages through a French pressure cell, the cell debris was removed by centrifugation and the supernatant cleared by ultrafiltration through a 0.45 µm device yielding 45 ml crude extract.

Protein purification was performed on an automated FPLC (Vision workstation, PE Biosystems) at room temperature. 10 ml of the crude extract were applied to a 1.7 ml Ni²⁺-charged MC-Poros column previously equilibrated with buffer A. The column was washed and the bound protein eluted with imidazole in a gradient from 0 to 300 mM in buffer A and immediately applied to a 10 ml StrepTactin-Sepharose column (IBA, Göttingen, Germany), equilibrated with buffer B (100 mM Tris/HCl pH 8.0, 1 mM EDTA). The column was washed and the protein of interest eluted by injecting 20 ml of 1 mM desthiobiotin (Sigma) in buffer B. The peak fractions were pooled (total volume 15 ml) and the buffer exchanged through a desalting column (HiPrep 26/10, Amersham Pharmacia) equilibrated with 20 mM Hepes/KOH pH 6.0, 20 mM NaCl. Finally, the sample was adjusted to a concentration of 20 mg/ml by ultrafiltration (cutoff 5 kDa, Millipore).

Fourier Transform Infrared Spectrometry

For Fourier transform infrared (FTIR) spectrometry, the protein samples were freeze-dried and re-diluted in D₂O containing 150 mM NaCl, yielding a concentration of 10 mg/ml. A pH of 7.5 was adjusted in each sample by adding a few microliters of diluted NaOH or HCl, respectively. About 50 µl of the protein were injected into a temperature-controlled 30 mm diameter transmission cell with two BaF₂ windows and a 50 µm polytetrafluorethylene gasket. The cell was placed in the sample chamber of a Bruker ifs 66-V, equipped with a LN₂-cooled HgMnTe detector (J15D series, EG&G Judson) and continuously flushed with

dry air. Prior to each sample measurement, reference buffer was filled into the freshly assembled chamber through injection ducts. A single beam spectrum was taken, then the buffer was removed and the protein sample was injected. The temperature was raised linearly ($\Delta T = 1$ K/min), spectra were taken every 5 K. The second derivatives of the difference spectra were calculated using the instrument software (Opus 3.0, Bruker Optik GmbH, Rheinstetten, Germany).

Automated protein crystallization

Initial crystallization conditions for His₆-SH3-StrepII were screened in hanging-drop vapor-diffusion mode in a 96-well microplate using a commercial screen (Hampton Research). The protein drops (1 µl droplet volume) were set on a 2D array on a compact glass substrate in less than 60 s using dispensing equipment developed in-house [17]. The screening solution of 1 µl was added rapidly by a multichannel pipetting robot Hydra (Robbins). In parallel, a standard 96-well microplate (655 101, Greiner) was filled with screening solutions of 150 µl each, using the same system. Taken together, the complete 96-condition screening plate was prepared in less than 3 min. The first crystals sized larger than 100 µm were detected after 4 days. After 22 days, additional crystals of various size and morphology appeared under six other screening conditions. For diffraction experiments, a crystal of 320 × 300 × 200 µm grown from 10% (by vol.) dioxane, 0.1 M MES pH 6.5, 1.6 M ammonium sulfate was harvested after 26 days.

X-ray diffraction, structure determination and refinement

X-ray diffraction data were collected on a MAR-Research imaging plate detector (300 mm diameter) mounted on a direct-drive Rigaku Denki RU H2R X-ray generator producing Cu-K α radiation. The crystal was cooled to 110 K after exchanging the surrounding mother liquor with paraffin oil [18]. Diffraction data processing statistics are shown in Table 1.

For structure solution by molecular replacement using AMORE [19], the SH3 domain of chicken α -spectrin [13], pdb entry 1SHG, served as a search model. It gave a clear solution in the cross rotation function with a signal-to-noise ratio of 4.82 for reflections from 8-4 Å. With an *R* value of 39.6% and a correlation coefficient of 0.62, the true space group, P4₃2₁2, could be easily distinguished from the other

Table 1. Diffraction data statistics.

Indexed space group	P4 ₁ 2 ₁ 2 / P4 ₃ 2 ₁ 2
Unit-cell dimensions (Å)	a = 41.86, c = 92.86
Radiation source	Rotating anode, Cu K _α radiation
Resolution range (Å)	31.0–2.3
Unique observations	3,858
Mosaicity (°)	0.721
Completeness ^a (%)	99.2 / 95.6
Redundancy	4.4
R _{sym} ^a	0.109 / 0.461
B from Wilson statistics (Å ²)	26.6
Mean I / σ(I) ^a	13.03 / 1.92
V _M (Å ³ /Da)	2.8
No. of molecules per asymmetric unit	1

^a All data / high resolution shell.

possible enantiomorph, P4₁2₁2 (*R* = 49.0%, corr. = 0.34), in the translation function.

CNS v 0.96 [20] was used for structure refinement. A stepwise improvement of the model was achieved starting with a rigid-body relaxation and subsequent simulated annealing with torsional dynamics calculation. After this initial stage, several rounds of positional refinement, individual *B*-factor refinement and manual model building led to the final model with a *R* value of 20.0% and *R*_{free} of 24.9%. Although the data quality was not excellent, 9 out of 11 C-terminal StrepII-tag residues could be easily placed in the difference electron density. The 12 N-terminal His₆-tag residues and the following residues 2–5 of the native polypeptide chain were not represented in the electron density, presumably due to flexibility of the N-terminus. Atomic coordinates and X-ray diffraction data were deposited with the Protein Data Bank [21], accession number 1NEG.

Results

Sample preparation for structure analysis

A 250-ml culture of the recombinant *E. coli* clone yielded 1.1 g of wet cell paste out of which 12 mg of His₆-SH3-StrepII were purified to electrophoretic homogeneity (Figure 2). The tandem configuration of the MC-Poros and StrepTactin affinity columns allowed the preparation of pure protein within two hours. Due to the speed of removal of contaminating

polypeptides, the use of protease inhibitors was not required. After desalting and concentration, the protein sample was ready for biophysical characterization and crystallization.

Fourier Transform Infrared Spectrometry

Fourier transform infrared (FTIR) spectrometry is widely used for protein structure analysis [22, 23]. The region between 1,600 and 1,700 cm⁻¹ in the FTIR spectrum is called the amide I band. Absorption in this region is mainly due to C=O stretching vibrations, slightly coupled with CN stretching, CCN deformation and NH bending vibrations [23]. The band position of the amide I band is strongly influenced by the formation of hydrogen bonds, because these interactions alter the force constants of donor as well as acceptor groups and influence the frequencies for their stretching and bending vibrations. Thus, the amide I position allows to distinguish between secondary structure elements that build up the overall structure of the protein [24].

Figure 3(a) (upper black curve) shows the second derivative of the amide I region for the untagged chicken α-spectrin SH3 domain. The most intense absorption at about 1,633 cm⁻¹, together with a very pronounced second maximum at 1,681 cm⁻¹, points to a high content (>80%) of β-sheet [24]. The presence of a small amount of α-helical conformations could be deduced from absorption bands between 1,646 and 1,660 cm⁻¹ [25]. In addition, there is a small absorption at 1,666 cm⁻¹, a wave number often reported for 3₁₀-helices [22].

The spectrum of His₆-SH3-StrepII is only slightly different from that of the untagged SH3 domain (see Figure 3(a), upper blue curve): The most intense absorption is shifted a little towards smaller wave numbers (1,628 cm⁻¹). This indicates a more compact structure of the β-barrel. At higher wave numbers the bands known from the untagged SH3 domain become less defined, presumably due to the presence of unordered regions within the affinity tags. Taken together, the tags seem to have only a slight influence on the secondary structure of the SH3 domain in solution.

We observe only small changes in the secondary structure of His₆-SH3-StrepII up to 70 °C (see Figure 3(a), lower black curve). In contrast, there are temperature-dependent changes in the untagged SH3 domain that result in a spectrum (lower blue curve in Figure 3(a)) similar to His₆-SH3-StrepII. The struc-

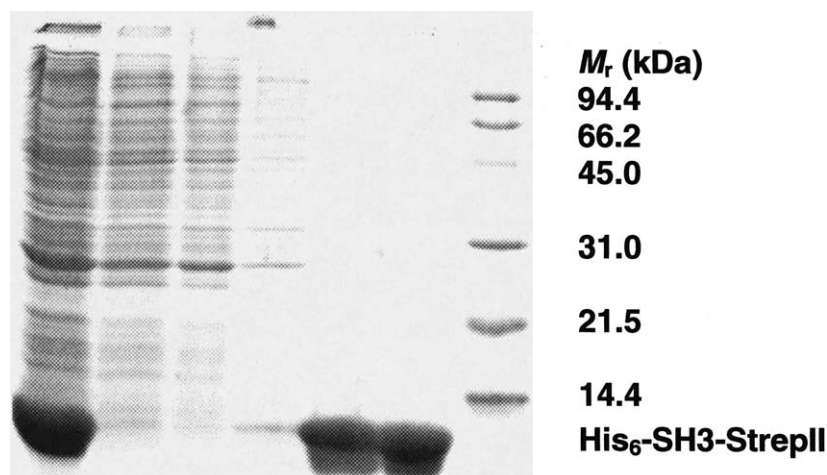


Figure 2. Affinity chromatography of His₆-SH3-StrepII, 15% SDS-PAGE. Lanes (from left): Crude cell extract, flowthrough fractions (3 ×), peak fractions from StrepTactin-Sepharose (2 ×), size standard.

ture becomes less ordered, as can be seen from the absorption at 1,648 cm⁻¹. Shown in greater detail in Figure 3(b) is the shift of the most intense absorption to 1,629 cm⁻¹ at 70 °C, reflecting the development of a structure as compact as that of His₆-SH3-StrepII. At temperatures above 70 °C the spectra of both protein variants display bands at around 1,615 cm⁻¹ and 1,678 cm⁻¹ characteristic for the formation of intermolecular hydrogen bonds between extended chains following denaturation or aggregation [22].

Crystal structure analysis

The structure of His₆-SH3-StrepII was determined at 2.3 Å resolution and refined against X-ray diffraction data from a laboratory source (Table 2). Residues Lys6 to Phe70 of the fusion protein (see Figure 1) are revealed by electron density. Thus, the N-terminal His₆ tag and five N-terminal residues of the SH3 domain are completely disordered in the crystal, whereas most residues of the C-terminal StrepII tag are structured and observed. Disorder of the N-terminal pentapeptide of the SH3 domain was observed earlier [13] and is thus not due to the presence of the His₆ tag. The partial order of the StrepII peptide is mainly due to intermolecular contacts between residues Leu61, His67 and Gln69 and residues Arg21, Lys43 and Gln50 of a neighboring molecule in the crystal lattice. With the exception of three residues, all backbone torsion angles are in the most preferred region of the Ramachandran diagram of PROCHECK [26]. Asn47, located in a turn between strands 2 and

Table 2. Refinement and model statistics.

Resolution limits (Å)	31.1–2.3
No. of reflections	3,858
Test set (10%)	382
<i>R</i> factor (%)	20.0
<i>R</i> _{free} factor (%)	24.9
Protein atoms	536
Solvent atoms	46
Other ligand atoms	1.5
Rms deviation from ideal values	
Bond lengths (Å)	0.011
Bond angles (°)	1.5
Dihedral angles (°)	26.3
Mean isotropic thermal factors	
Main-chain atoms (Å ²)	22.5
Side-chain atoms (Å ²)	26.1
All protein atoms (Å ²)	24.5
Solvent atoms (Å ²)	34.7

3, is unique in adopting ϕ/ψ values that fall in the generously allowed part of the plot. This was observed earlier in the crystal structure of the chicken α -spectrin SH3 domain [13] where Asn47 resides in the disallowed region of the ϕ/ψ diagram. The electron density prompted us to model three residues (Lys26, Lys60 and Gln69) with two alternative side-chain conformations and to include 48 water molecules and one ion into the model.

As expected, His₆-SH3-StrepII displays the typical fold of a SH3 domain which is characterized by the antiparallel pairing of five β -strands interspersed by loops of varying length (Figure 4). The three-resi-

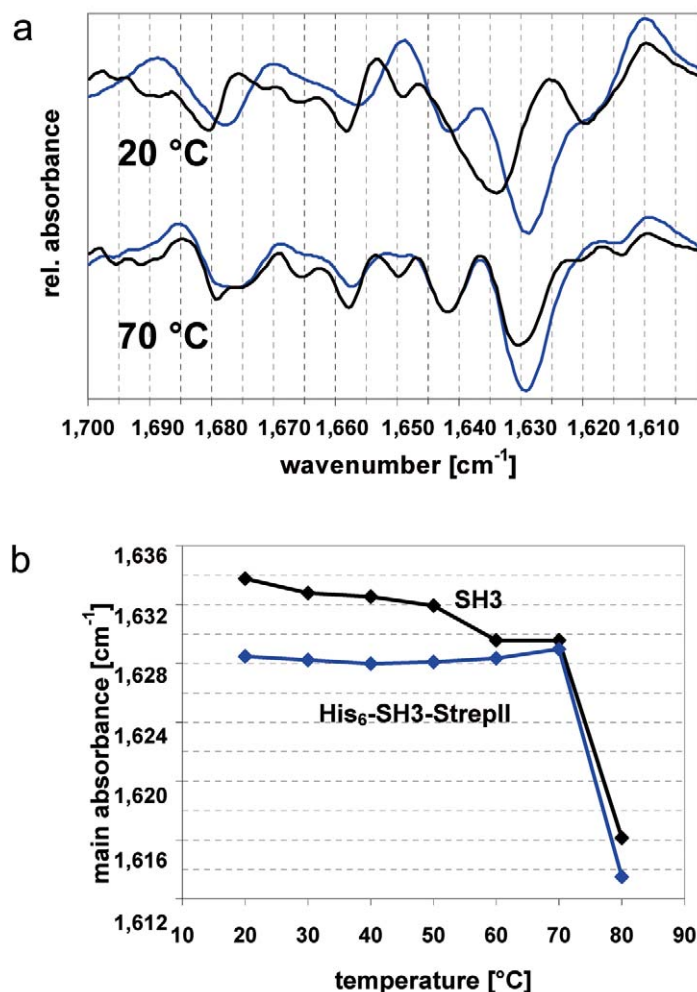


Figure 3. (a) Secondary structure elements of the SH3 domain with and without affinity tags. Temperature-controlled second-derivative FTIR spectra (amide I region) of His₆-SH3-StrepII (blue curves) and the untagged SH3 domain (black curves) at 20 °C (upper panel) and 70 °C (lower panel), respectively. Freeze-dried protein samples were re-diluted in D₂O containing 150 mM NaCl and adjusted to pH 7.5. Measurements were carried out in a transmission cell under aeration with dried air. (b) Temperature-dependent changes of the main absorption band in the FTIR spectra of the SH3 domain with and without affinity tags.

due 3₁₀-helix between β -strands 4 and 5 of His₆-SH3-StrepII is found in nearly all SH3 domains studied so far [27, 28]. An elongated difference density (see Figure 4) atop a crystallographic twofold axis between two protein molecules was interpreted as a half occupied azide anion. This interpretation is based on the form of the density which accommodates the linear azide very well and the vicinity of two positive charges from the symmetry-equivalent Lys59 residues.

In a least-squares fit, the C α atoms of His₆-SH3-StrepII superimpose onto the matching atoms of the

chicken α -spectrin SH3 domain (1SHG, ref. 13) with a rms deviation of 0.44 Å, and all equivalent atoms of the two structures superimpose with a rms deviation of 1.08 Å. The secondary structure elements are particularly well conserved between the molecules (see Figure 4). Thus, the two crystal structures are nearly identical within the error limits of the structure analyses at 2.3 Å and 1.8 Å resolution, respectively, and considering the packing in different crystal lattices. We note, in addition, that there is no systematic difference between the structures near the ends of the polypeptide chains where the tags present in His₆-

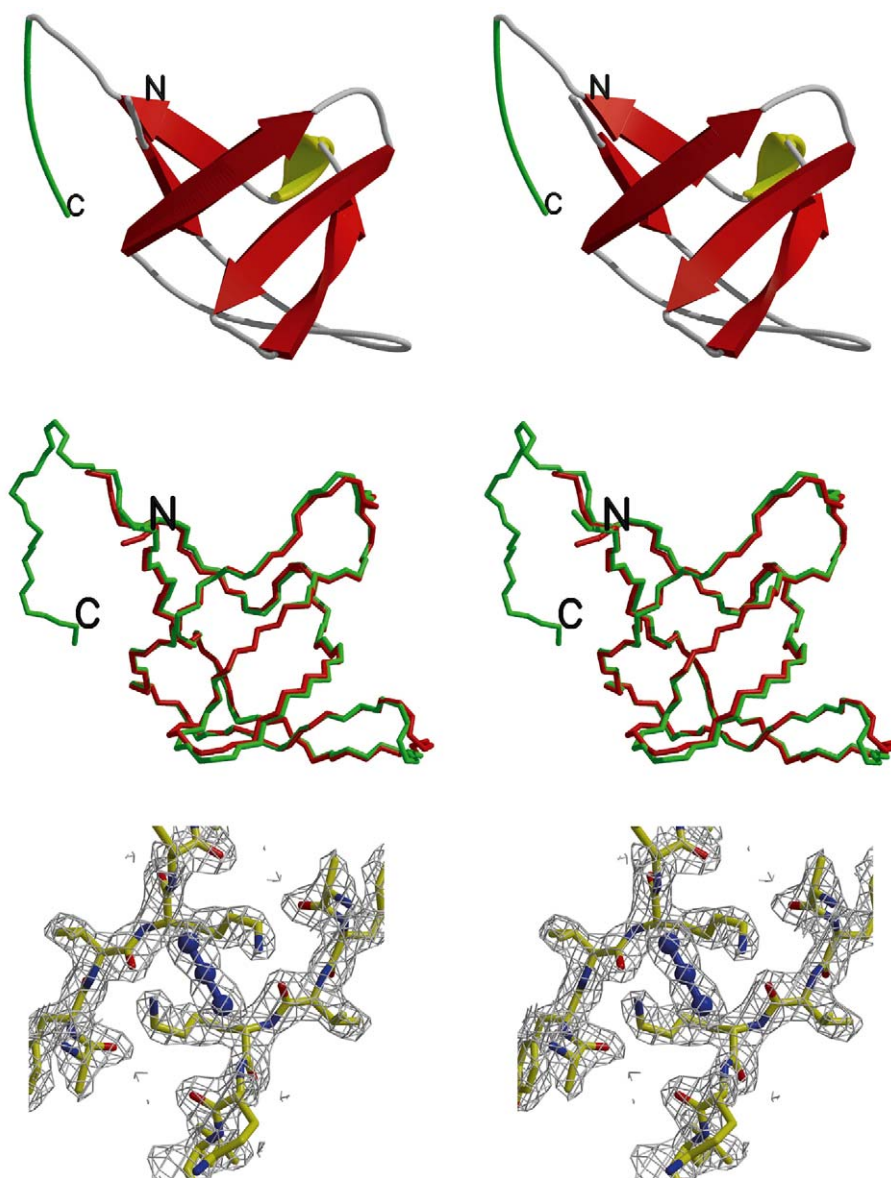


Figure 4. Crystal structure of His₆-SH3-StrepII. Top: Schematic drawing of the structure. The course of the polypeptide chain is depicted as a grey wire, red arrows indicate β -strands, and the signature 3_{10} -helix between strands 4 and 5 of the SH3 domain is shown in yellow color. Green color indicates the portion of the protein backbone belonging to the C-terminal StrepII tag. Middle: Least-squares superposition of the backbones of His₆-SH3-StrepII and the crystal structure of the chicken α -spectrin SH3 domain (1SHG, ref. 123). Bottom: $2F_o - F_c$ density (grey, contoured at 1.5σ) with a part of the final model. The density at the figure center was interpreted as an azide ion residing on a crystallographic dyad axis.

SH3-StrepII might be suspected to distort the molecular geometry. Finally, we wish to point out that the slightly worse resolution of the X-ray data obtained from the His₆-SH3-StrepII crystal may be due to the

X-ray source (rotating anode *versus* synchrotron beamline as used for the SH3 data collection [13]) and thus cannot or cannot fully be attributed to the presence of the purification tags.

Discussion

Speeding up the production of crystallizable protein is a core issue in every structural genomics project or high-throughput structure analysis scheme [29–31]. Among the approaches towards this end adopted by the Protein Structure Factory [11, 12] is the dual affinity tagging of proteins with a His₆ [14] and a StrepII [15, 16] peptide epitope. This strategy was chosen for a number of reasons and has been tested with a set of human proteins recombinantly produced in either *E. coli* or yeast. So far, it has been observed that the cost-effective N-terminal His₆ tag usually affords an electrophoretic purity between 90 and 95% in the initial purification step. Since this is considered insufficient for crystallization and structure analysis, it is vital to add a second affinity chromatographic step for fast and efficient protein purification. As described above, we have chosen a C-terminal StrepII tag to serve this purpose. Using a C-terminal tag ensures that only full-length proteins are purified. The combination of the two affinity chromatographies allows for fast, reliable and easily automatable protein preparation. A time-consuming optimization of additional chromatographic steps according to the properties of individual proteins and cost- and labor-intensive proteolytic treatments with the accompanying risk of degrading the protein are avoided. To further increase the throughput in protein purification, it may be necessary and possible to run the described protocol with many samples in parallel, perhaps in a 96-well format with the perspective to automate the whole procedure as recently described by several authors [32–34].

One concern when working with affinity-tagged proteins is that the peptide epitopes added to the natural polypeptide chain termini might interfere with crystallization due to their inherent flexibility. In the case of His₆-SH3-StrepII, this concern proved unfounded. Crystals were obtained from 8 out of 96 tested screen conditions [35], and the structure analysis was carried out with a crystal taken directly from the primary screen without further optimization. We thus demonstrate that protein crystallization and structure analysis are indeed possible with affinity-tagged proteins, even in the extreme case where more than one fourth of the fusion protein mass originates from two peptide tags. We do not intend to suggest that this approach will always yield the desired result, i.e. well diffracting single crystals. It is well documented [36] that the removal of peptide tags may be

beneficial for crystallization of certain proteins. On the other hand, there have been a few examples of proteins that crystallized better when fused to molecules used for affinity purification [10]. Our suggestion is that constructs such as the His₆-SH3-StrepII presented here may be a good starting point for high-throughput structure analysis, since they permit easy and automatable protein purification and can, in principle, be crystallized. In recent work, we have been able to grow diffraction-quality crystals of several other affinity-tagged proteins.

The additional concern that the affinity tags might alter the protein structure in an unnatural way also proved unfounded in the case of His₆-SH3-StrepII. The crystal structure showed its SH3 domain to be virtually indistinguishable from the unmodified SH3 domain [13]. The infrared spectra we measured for the proteins in solution serve as a control for this observation. They, too, reveal only slight differences between both protein forms that can well be explained by contributions of the tags to the overall secondary structure that are independent of the protein core. There are scattered reports in the literature of other proteins, the structures of which remained unchanged when purification tags were added to the wildtype form [37, 38]. Our main finding is that this remains true, even if the tags represent a considerable fraction of the total protein mass. Hence, the use of two short terminal peptide tags should be considered as an option for affinity purification of proteins for structural studies, since it permits highly efficient protein purification and may neither interfere with crystallization nor change the conformation of the protein of interest.

Acknowledgement

The generation and testing of expression constructs by J. Tischer is gratefully acknowledged. This work was funded by the German Ministry for Education and Research through the Leitprojektverbund 'Proteinstrukturfabrik'. Support of this work by the Berlin Senate, the European Fund for Regional Development (EFRE) and the Fonds der Chemischen Industrie is also gratefully acknowledged.

References

1. Burley, S.K. (2000) *Nature Struct. Biol.* **7**, 932–934.

2. Stevens, R.C., Yokoyama, S. and Wilson, I.A. (2001) *Science* **294**, 89–92.
3. Terwilliger, T.C. (2000) *Nature Struct. Biol.* **7**, 935–939.
4. Heinemann, U. (2000) *Nature Struct. Biol.* **7**, 940–942.
5. Yokoyama, S., Hirota, H., Kigawa, T., Yabuki, T., Shirouzo, M., Terada, T., Ito, Y., Matsuo, Y., Kuroda, Y., Nishimura, Y., Kyogoku, Y., Miki, K., Masui, R. and Kuramitsu, S. (2000) *Nature Struct. Biol.* **7**, 943–945.
6. Abola, E., Kuhn, P., Earnest, T. and Stevens, R.C. (2000) *Nature Struct. Biol.* **7**, 973–977.
7. Heinemann, U., Illing, G. and Oschkinat, H. (2001) *Curr. Opin. Biotechnol.* **12**, 348–354.
8. Blundell, T.L., Jhoti, H. and Abell, C. (2002) *Nature Rev. Drug Discov.* **1**, 45–54.
9. Jhoti, H. (2001) *Trends Biotechnol.* **19**, S67–S71.
10. Kuge, M., Fujii, Y., Shimizu, T., Hirose, F., Matsukage, A. and Hakoshima, T. (1997) *Protein Sci.* **6**, 1783–1786.
11. Heinemann, U., Frevert, J., Hofmann, K. P., Illing, G., Maurer, C., Oschkinat, H. and Saenger, W. (2000) *Prog. Biophys. Mol. Biol.* **73**, 347–362.
12. Heinemann, U. (2002) *Gene Funct. Dis.* **3**, 25–32.
13. Musacchio, A., Noble, R., Pauptit, R., Wierenga, R. and Saraste, M. (1992) *Nature* **359**, 851–855.
14. Hochuli, E., Bannwarth, W., Dobeli, H., Gentz, R. and Stüber, D. (1988) *Biotechnology* **6**, 1321–1325.
15. Schmidt, T.G. and Skerra, A. (1994) *J. Chromatogr. A* **676**, 337–345.
16. Schmidt, T.G.M., Koepke, J., Frank, R. and Skerra, A. (1996) *J. Mol. Biol.* **255**, 753–766.
17. Mueller, U., Nyarsik, L., Horn, M., Rauth, H., Przewieslik, T., Saenger, W., Lehrach, H. and Eickhoff, H. (2001) *J. Biotechnol.* **85**, 7–14.
18. Riboldi-Tunicliffe, A. and Hilgenfeld, R. (1999) *J. Appl. Crystallogr.* **32**, 1003–1005.
19. Navaza, J. (1994) *Acta Crystallogr. A* **50**, 157–163.
20. Brünger, A.T., Adams, P.D., Clore, G.M., DeLano, W.L., Gros, P., Grosse-Kunstleve, R.W., Jiang, J.-S., Kuszewski, J., Nilges, M., Pannu, N.S., Read, R.J., Rice, L.M., Simonson, T. and Warren, G.L. (1998) *Acta Crystallogr. D* **54**, 905–921.
21. Berman, H.M., Bhat, T.N., Bourne, P.E., Feng, Z., Gilliland, G., Weissig, H. and Westbrook, J. (2000) *Nature Struct. Biol.* **7**, 957–959.
22. Jackson, M. and Mantsch, H.H. (1995) *Crit. Rev. Biochem. Mol. Biol.* **30**, 95–120.
23. Jung, C. (2000) *J. Mol. Recogn.* **13**, 325–351.
24. Cooper, E.A. and Knutson, K. (1995) In: *Physical Methods to Characterize Pharmaceutical Proteins*, Herron, J.N. (Ed.), Plenum Press, New York, pp. 101–141.
25. Bylar, D.M. and Susi, H. (1986) *Biopolymers* **25**, 469–487.
26. Laskowski, R.A., MacArthur, M.W., Moss, D.S. and Thornton, J.M. (2002) *J. Appl. Crystallogr.* **26**, 283–291.
27. Musacchio, A., Wilmanns, M. and Saraste, M. (1994) *Prog. Biophys. Mol. Biol.* **61**, 283–297.
28. Delbrück, H., Ziegelin, G., Lanka, E. and Heinemann, U. (2002) *J. Biol. Chem.* **277**, 4191–4198.
29. Terwilliger, T.C. and Berendzen, J. (1999) *Acta Crystallogr. D* **55**, 849–861.
30. Christendat, D., Yee, A., Dharamsi, A., Kluger, Y., Savchenko, A., Cort, J.R., Booth, V., Mackereth, C.D., Saridakis, V., Ekiel, I., Kozlov, G., Maxwell, K.L., Wu, N., McIntosh, L.P., Gehring, K., Kennedy, M.A., Davidson, A.R., Pai, E.F., Gerstein, M., Edwards, A.M. and Arrowsmith, C.H. (2000) *Nature Struct. Biol.* **7**, 903–909.
31. Edwards, A.M., Arrowsmith, C.H., Christendat, D., Dharamsi, A., Friesen, J.D., Greenblatt, J.F. and Vedadi, M. (2000) *Nature Struct. Biol.* **7**, 970–972.
32. Nasoff, M., Bergseid, M., Hoeffler, J.P. and Heyman, J.A. (2000) *Methods Enzymol.* **328**, 515–529.
33. Albala, J.S., Franke, K., McConnell, I.R., Pak, K.L., Folta, P.A., Rubinfeld, B., Davies, A.H., Lennon, G.G. and Clark, R. (2000) *J. Cell. Biochem.* **80**, 187–191.
34. Gilbert, M. and Albala, J.S. (2002) *Curr. Opin. Chem. Biol.* **6**, 102–105.
35. Jancarik, J. and Kim, S.-H. (1991) *J. Appl. Crystallogr.* **24**, 409–411.
36. Bucher, M.H., Evdokimov, A.G. and Waugh, D.S. (2002) *Acta Crystallogr. D* **58**, 392–397.
37. Steipe, B., Plückthun, A. and Huber, R. (1992) *J. Mol. Biol.* **225**, 739–753.
38. Schubert, H.L., Wilson, K.S., Raux, E., Woodcock, S.C. and Warren, M.J. (1998) *Nature Struct. Biol.* **5**, 585–591.